Acta Montanistica Slovaca
ISSN 1335-1788
actamont.tuke.sk

Application of resistance strain gauges to determine stresses on the tooth flanks of toothed segments of the KOMTRACK advance system of a longwall shearer

Marek KALITA[1], Dominik BAŁAGA[2], Michał SIEGMUND[3], Krzysztof KACZMARCZYK[4], Krzysztof NIEŚPIAŁOWSKI[5], Andrzej NIEDWOROK[6] and Andrzej N. WIECZOREK[7]*

Authors' affiliations and addresses:
[1] KOMAG Institute of Mining Technology, Division of Machinery and Equipment,
37 Pszczyńska str., 44-101 Gliwice, Poland
e-mail: mkalita@komag.eu

[2] KOMAG Institute of Mining Technology, Division of Machinery and Equipment,
37 Pszczyńska str., 44-101 Gliwice, Poland
e-mail: dbalaga@komag.eu

[3] KOMAG Institute of Mining Technology, Division of Machinery and Equipment,
37 Pszczyńska str., 44-101 Gliwice, Poland
e-mail: msiegmund@komag.eu

[4] KOMAG Institute of Mining Technology, Division of Machinery and Equipment,
37 Pszczyńska str., 44-101 Gliwice, Poland
e-mail: kkaczmarczyk@komag.eu

[5] KOMAG Institute of Mining Technology, Division of Machinery and Equipment,
37 Pszczyńska str., 44-101 Gliwice, Poland
e-mail: kniespialowski@komag.eu

[6] KOMAG Institute of Mining Technology, Laboratory of Applied Tests, 37 Pszczyńska str., 44-101 Gliwice, Poland
e-mail: aniedworok@komag.eu

[7] Silesian University of Technology, Faculty of Mining and Geology, 2A Akademicka str., 44-100 Gliwice, Poland
e-mail: andrzej.n.wieczorek@polsl.pl

***Correspondence:**
Marek Kalita, KOMAG Institute of Mining Technology, Division of Machinery and Equipment, 37 Pszczyńska str., 44-101 Gliwice, Poland
tel.: +48 32 23 74 628
e-mail: mkalita@komag.eu

Funding information:
The article was based on the results of the tests carried out within the research project entitled "New generation high-performance haulage system of the longwall system" co-financed by the European Regional Development Fund (Contract no. POIR.04.01.04-00-0068/17).

How to cite this article:
Kalita, M., Bałaga, D., Siegmund, M., Kaczmarczyk, K., Nieśpiałowski, K., Niedworok, A. and Wieczorek, A.N. (2025). Application of resistance strain gauges to determine stresses on the tooth flanks of toothed segments of the KOMTRACK advance system of a longwall shearer. *Acta Montanistica Slovaca*, Volume 30 (4), 845-863

DOI:
https://doi.org/10.46544/AMS.v30i4.02

Abstract
Issues related to the general design and purpose of shearer advance systems, taking into account key historical solutions and global experience gained from the operation of longwall systems in underground mines, are presented. Currently used shearer advance systems are based on chainless systems with a toothed drive wheel cooperating with toothed bars mounted in the chain conveyor troughs. This design, in different variants, is used in many countries as the primary system responsible for moving the shearer along the mining face. Despite its many advantages, the Eicotrack advance system also has a disadvantage resulting from the rigid design of the toothed bars. These disadvantages are accentuated by premature wear of the gear teeth and toothed bars, especially on non-linear sections of the longwall conveyor route. As part of the KOMTRACK research project, co-financed by the European Regional Development Fund, an attempt was made to develop an innovative advanced system with the flexibility and adaptability of toothed segments mounted in guides to the current position of the gang wheel. In addition to design work, a number of studies were conducted using various testing techniques. One of the research directions was to determine approximate stress values at the contact surface between the toothed segment and the gang wheel tooth using resistance strain gauges. The testing methodology and the results, along with their analysis, are presented. It has been concluded that the developed testing methodology, based on resistance strain gauges, can be successfully used to identify stresses at the contact surface of the friction pair formed by the gear wheel tooth and the tooth of the toothed segment. Stresses determined from the measured strains for a single gear wheel provide repeatable results after approximately twenty contacts between the gear wheel and the gear segment. A higher number of loads results in the strain gauge system becoming decalibrated, leading to significant discrepancies in the results or a loss of the strain gauges' measurement capabilities.

Keywords
shearer haulage system, flexible collaboration, strain gauge, stress, strength tests, toothed segment.

Introduction

Longwall shearers used in hard coal mining are equipped with a haulage system that allows the machine to move along the mining face and to load the mined material. Over the fifty-year history of longwall shearer operation, chainless haulage systems with a toothed or pin-type drive wheel have been tested (Mackie et al., 1987; Langefeld & Paschedag, 2019; Sikora et al., 2003; Korski, 2021A), as well as systems such as Rackatrack, Peratrack, and Dynatrack, described in publications such as (Korski, 2021B; Fennelly, 1978; Braun, 1983). Currently, chainless haulage systems such as Eicotrack, Megatrack, and Gigatrack are widely used in hard coal mines, and their design and operating principles are described in publications (Sikora et al., 2005; Korski, 2020; Fries, 2003). These systems, commonly used, have a number of advantages and a major disadvantage resulting from the rigid design of the toothed bars (Kotwica et al., 2023; Giza & Mann, 2005; Piekło et al., 2016; Giza et al., 2003), the unfavorable features of which are demonstrated by premature wear of the teeth of the gang wheels and the pins in the toothed bars on non-linear sections of the face conveyor route (Twardoch et al., 2016; Kotwica et al., 2021; Kovanič et al., 2021). The rigid attachment of the toothed bar segments (ladders) to the gate supports prevents their movement, especially in the horizontal plane, which changes the position of the toothed bar relative to the gang wheel during bending of the scraper conveyor route. This leads, on one hand, to a disturbance of the pitch between the extreme pins of adjacent ladders and a change in the distance between the pins of the toothed bar segments and the axis of rotation of the gang wheel. These unfavorable phenomena, in turn, lead to so-called tooth edging, which results in excess dynamic forces that increase wear on the shearer gang wheel. On the other hand, tooth edge wear significantly exceeds the pressure stress values at the mating surfaces of the gang wheel and the rack, leading to excessive wear of the gang wheel on shearer loaders. These phenomena have been intensified with increasing drivetrain power and shearer weight (Zachura & Żuczek, 2014; Kovanič et al., 2023; Gondek et al., 2000; Matsui & Shimada, 1996).

As part of the KOMTRACK research project carried out jointly by the KOMAG Institute of Mining Technology, the AGH University of Science and Technology, the Łukasiewicz Research Network – Krakow Institute of Technology, Specodlew Innowacyjne Przedsiębiorstwo Odlewnicze and the Polish Mining Group S.A., co-financed by the European Regional Development Fund (contract no. POIR.04.01.04-00-0068/17), an innovative advance system was developed, characterized by flexibility (Kotwica et al., 2023) and the ability to adjust the toothed segments installed in the guides to the current position of the gang wheel (Fig. 1).

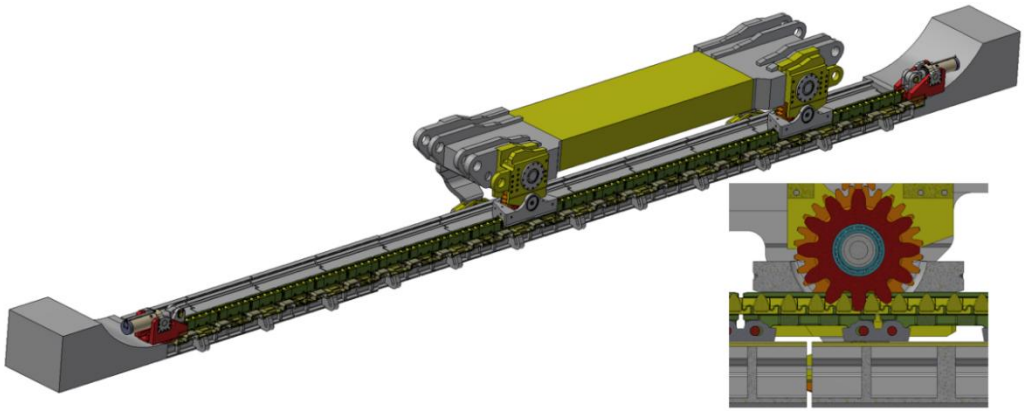

Fig. 1. KOMTRACK advancing system – cooperation of the shearer track wheel with the tooth segment

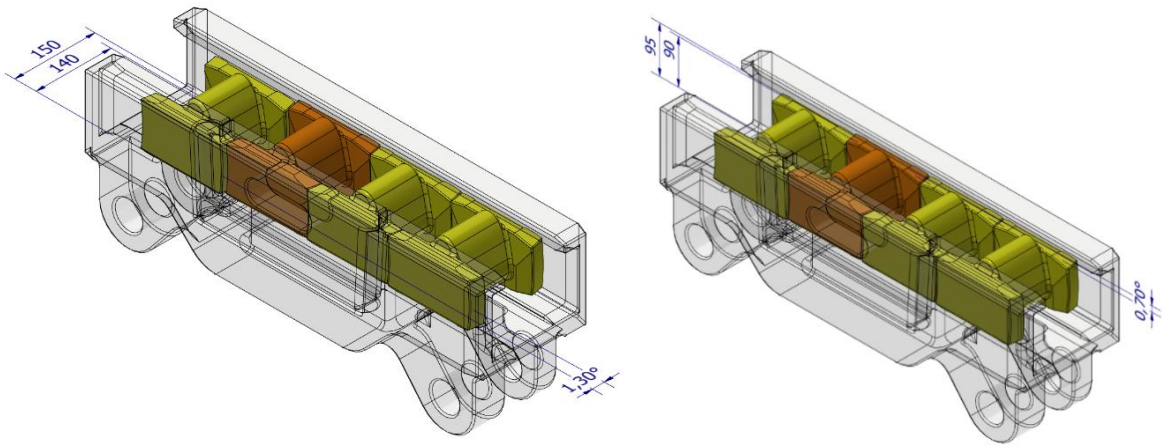

Fig. 2. Yield of the KOMTRACK advancing system: a) horizontal plane, b) vertical plane

The KOMTRACK system consists of guides attached to the conveyor trough and toothed segments placed in it. This system offers an advantage over previously used advancing systems as it allows the toothed segments to move relative to each other. This mobility in the horizontal and vertical planes, without changing the pitch, is enabled by toothed segments that contact each other with spherical surfaces. (Fig. 2).

In the KOMTRACK project, tests were planned to understand the nature of the friction pair between the gear wheel and the toothed segment, using strain gauges (Roliński, 1981; Iriarte et al., 2021). The friction pair in the advancing system has a contact across the mesh width, as is the case with gear transmissions (Shanran et al., 2023; Lingaiah & Ramachandra, 1977; Huang & Su, 2013). Therefore, the use of strain gauges as a method for determining stresses at the friction pair contact point is not possible due to damaging (crushing) the strain gauges. The problem of determining stresses in gear teeth is extensively discussed in (Park et al., 2024; Paucker et al., 2019; Zuo et al., 2025; Raghuwanshi & Parey, 2016; Syzrantsev & Syzrantsev, 2017; Link et al., 2013; Lisle et al., 2017; Lisle et al., 2019). In these papers, the authors present results from strain-gauge measurements of stresses at the tooth base, without addressing the problem of determining stresses at the tooth contact surface. To determine the actual stresses in the toothed segment resulting from the gang wheel's action, a simplification was applied, as shown in Fig. 3.

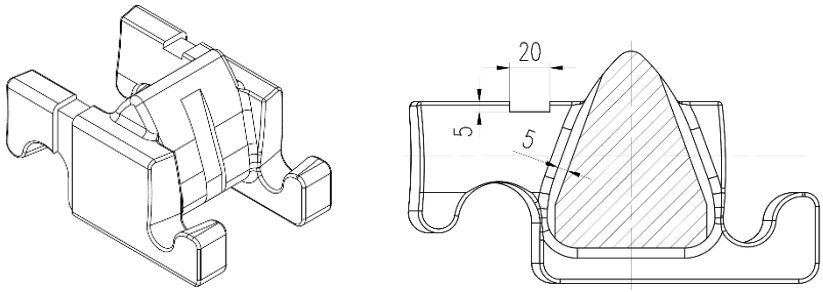

Fig. 3. Toothed segment prepared for gluing strain gauges on the side guides and on the tooth flank

For testing purposes, indentations in the toothed segment of the advancing system were made, both on the side guides and in the center of the tooth flank. These indentations allowed for the attachment of strain gauges, positioned and oriented in the direction of strain measurement, along with the routing of electrical cables, as shown in Fig. 4.

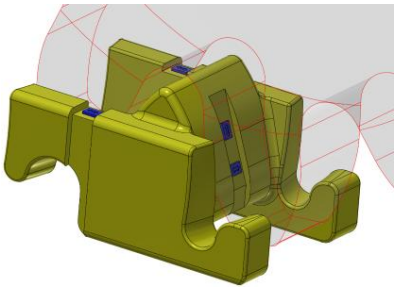

Fig. 4. Arrangement and orientation of strain measurement directions

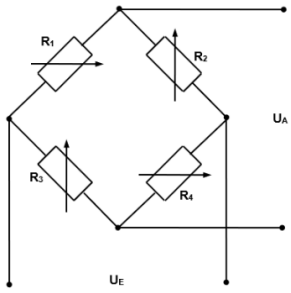

Fig. 5. Wheatstone bridge diagram

Measuring systems containing resistance strain gauges consist of an input circuit, an amplifier, and an output circuit that interfaces with sensitive devices that record changes in the resistance of the measuring components. Most often, the input circuit, including the strain gauges and the power supply, is implemented in a bridge configuration. To enable further processing and analysis of the signals coming from the bridge, an amplifier is used in the measuring line. When analyzing the operation of half-bridge strain gauge systems, it is convenient to consider a full Wheatstone measuring bridge (Roliński, 1981; Hoffman, 1989; Jung, 2022; Kitchin, 2004) (Fig. 5).

The bridge, supplied with constant voltage U_E, produces a voltage U_A at its output, described by the following relationship (1):

$$\frac{U_A}{U_E} = \left(\frac{R_1}{R_1+R_2} - \frac{R_3}{R_3+R_4}\right) \tag{1}$$

The initial resistance of the strain gauges $R_1 \div R_4$ is the same and equal to R. After setting the strain gauge resistance increment (due to deformations), the relationship (1) can take the following form (2):

$$\frac{U_A}{U_E} = \frac{1}{4}\left(\frac{\Delta R_1}{R_1} - \frac{\Delta R_2}{R_2} + \frac{\Delta R_3}{R_3} - \frac{\Delta R_4}{R_4}\right) \tag{2}$$

In the half-bridge circuit, only strain gauges R_1 and R_3 remain active. For the remaining ones, the resistance increase is constant and equal to 0 for the entire processing range. With this assumption, relationship (2) can take the following form (3):

$$\frac{U_A}{U_E} = \frac{1}{4}\left(\frac{\Delta R_1}{R_1} + \frac{\Delta R_3}{R_3}\right) \tag{3}$$

Further analysis should be performed for two cases:
- for a single active strain gauge (used in the measurements),
- for two active strain gauges.

For two active strain gauges, equation (3) remains unchanged, while for a single active strain gauge, equation (3) takes the following form (4):

$$\frac{U_A}{U_E} = \frac{1}{4}\left(\frac{\Delta R_1}{R_1}\right) \tag{4}$$

Since all strain gauges in the half-bridge configuration have the same characteristic resistance, it can be assumed that $R_1 = R_3 = R$. Thus, it can be assumed that for a single active strain gauge, equation (4) takes the following form (5):

$$\frac{U_A}{U_E} = \frac{1}{4}\left(\frac{\Delta R}{R}\right) \tag{5}$$

For two active strain gauges, equation (3) can be written in the following form (6):

$$\frac{U_A}{U_E} = \frac{1}{2}\left(\frac{\Delta R}{R}\right) \tag{6}$$

Using the relationships (5) and (6), we can determine the relative deformation ε. For the case where a single strain gauge is active, the relationship for relative deformation takes the following form (7):

$$\varepsilon = \frac{4}{k} \cdot \frac{U_A}{U_E} \tag{7}$$

However, for a system of two active strain gauges, the relative deformation takes the following form (8):

$$\varepsilon = \frac{2}{k} \cdot \frac{U_A}{U_E} \tag{8}$$

where:

ε – relative deformation,

k – strain gauge constant (for TF-5/120 strain gauges, it was 2.15 ± 0.5%).

According to Hooke's Law (9):

$$\sigma = E \cdot \varepsilon \tag{9}$$

where:

ε – relative deformation,

E –Young's modulus (modulus of longitudinal elasticity),

and by substituting equations (7) or (8) into it, one can determine the relationship defining the stresses expressed:

for a single active strain gauge (10):

$$\sigma = E \cdot \frac{4}{k} \cdot \frac{U_A}{U_E} \tag{10}$$

for two active strain gauges (11):

$$\sigma = E \cdot \frac{2}{k} \cdot \frac{U_A}{U_E} \tag{11}$$

Test stand and methodology of testing using the resistance strain gauges

Functional tests of the KOMTRACK haulage system required the development of a test stand, testing methodology, and appropriate preparation of the gear segments. The test methodology involved successive travels of the shearer loader along the KOMTRACK track and recording the selected physical parameters. It was assumed that the interaction between the gang wheel and the gear segments would be continuously monitored during the tests, via video recording of most runs. During each travel, the shearer was braked by a winch brake installed at the beginning of the route. The return travel was without the load.

The functional tests were planned for two main aspects. The first aspect of the tests was to verify the correct operation of the haulage system through successive runs along the shearer track, braked by the winch brake. The second aspect of the tests was to determine the stress values generated at selected locations on the gear segments due to contact with the gang wheel using strain-gauge measurements. In the case of measurements using resistance strain gauges, the number of travels was of secondary importance. The most important factor was to obtain the measurement data from the strain gauges and other sensors, recorded on a common time axis.

The program assumed tests on three tracks: a straight track, symbolically marked P (Fig. 6), a track with a horizontal bend, marked S (Fig. 7), and a track with a vertical bend, marked G (Fig. 8).

Fig. 6. Test track of straight profile P

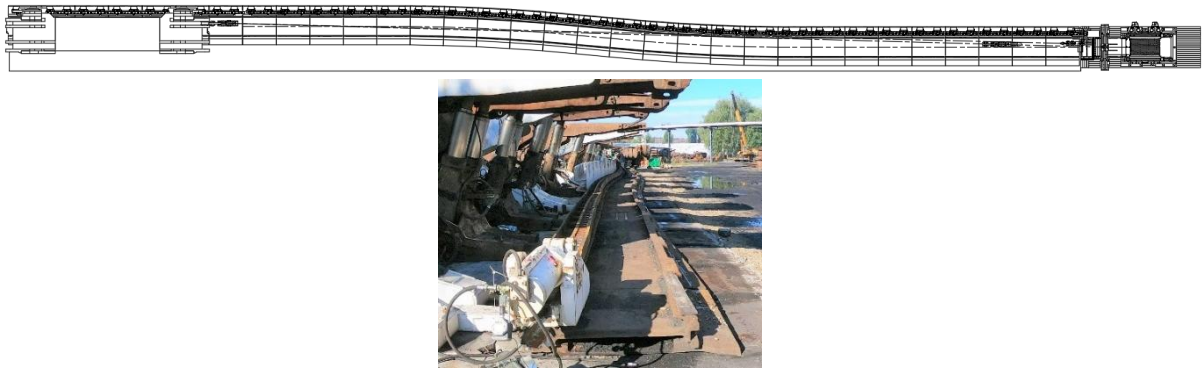

Fig. 7. Test track with a profile bent in the horizontal plane S

Fig. 8 Test track with a profile bent in the vertical plane G

For the tests, a ~50-meter-long section of the longwall complex equipped with the KOMTRACK haulage system was prepared at the storage yard of the Piast-Ziemowit coal mine (Ruch Piast). The toothed segments were placed in 66 guides. The guides, in turn, were attached to the conveyor troughs. Powered roof supports were installed along the length of the complex, enabling shaping of the shearer route profile. The complex was equipped

with a KSW-1140 longwall shearer manufactured by FAMUR S.A. The shearer haulage system was equipped with hydraulic tensioning systems located at both ends of the route.

Resistance strain gauge tests first required properly preparing the toothed segments and applying strain gauges to their surfaces. A total of 44 toothed segments were prepared for resistance strain gauge tests. (Fig. 9).

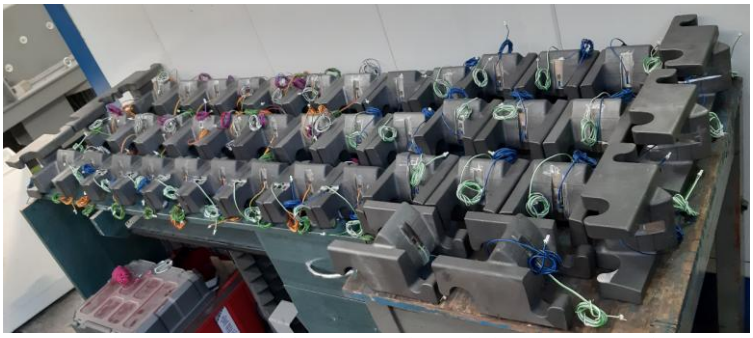

Fig. 9. Toothed segments prepared for testing with attached strain gauges and signal cables

Three types of toothed segments were prepared for strain gauge testing. Some were equipped with two strain gauges mounted on the tooth flank surface interacting with the gang wheel (Fig. 10).

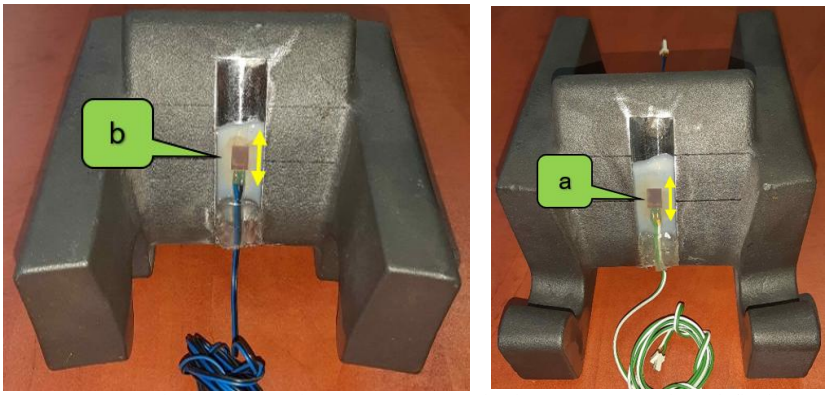

Fig. 10. Toothed segment with two strain gauges glued on it (one on each tooth flank)

Some were equipped with four strain gauges, mounted on each side of the surface in contact with the gang wheel (Fig. 11).

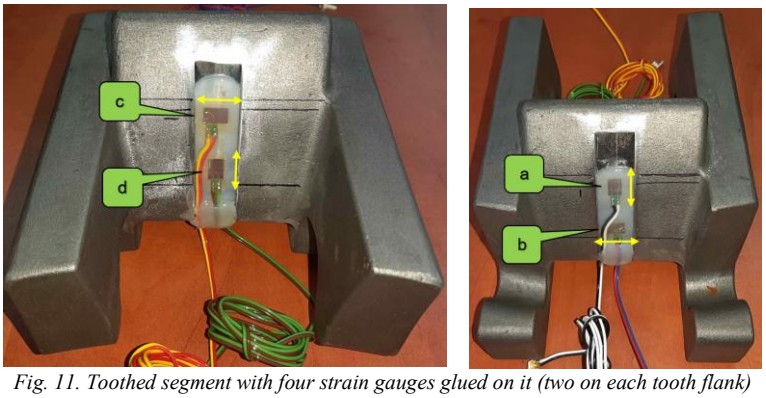

Fig. 11. Toothed segment with four strain gauges glued on it (two on each tooth flank)

The last type consisted of the segments with six strain gauges (Fig. 12), which, in addition to being mounted on the tooth flank, also had strain gauges on the side guides.

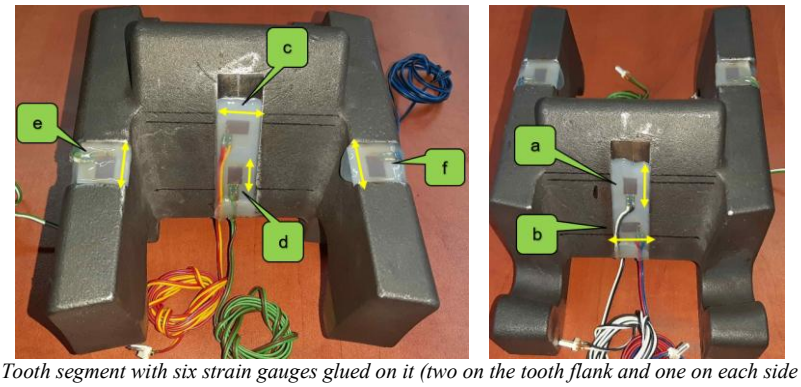

Fig. 12. Tooth segment with six strain gauges glued on it (two on the tooth flank and one on each side surface)

As part of the preparatory work for the tests, the strain gauges were connected with signal cables and plugs, which significantly simplified assembly of the measuring lines on the test stand. Furthermore, to protect the strain gauges and soldered joints from atmospheric conditions (especially moisture), appropriate adhesive coatings and additional silicone sealants were applied.

In parallel with the process of preparing the gear segments for testing, analytical work was conducted to determine the installation locations for the gear segments equipped with strain gauges in the track. Taking all boundary conditions into account, the installation locations for each gear segment were determined according to the diagram shown in Fig. 13.

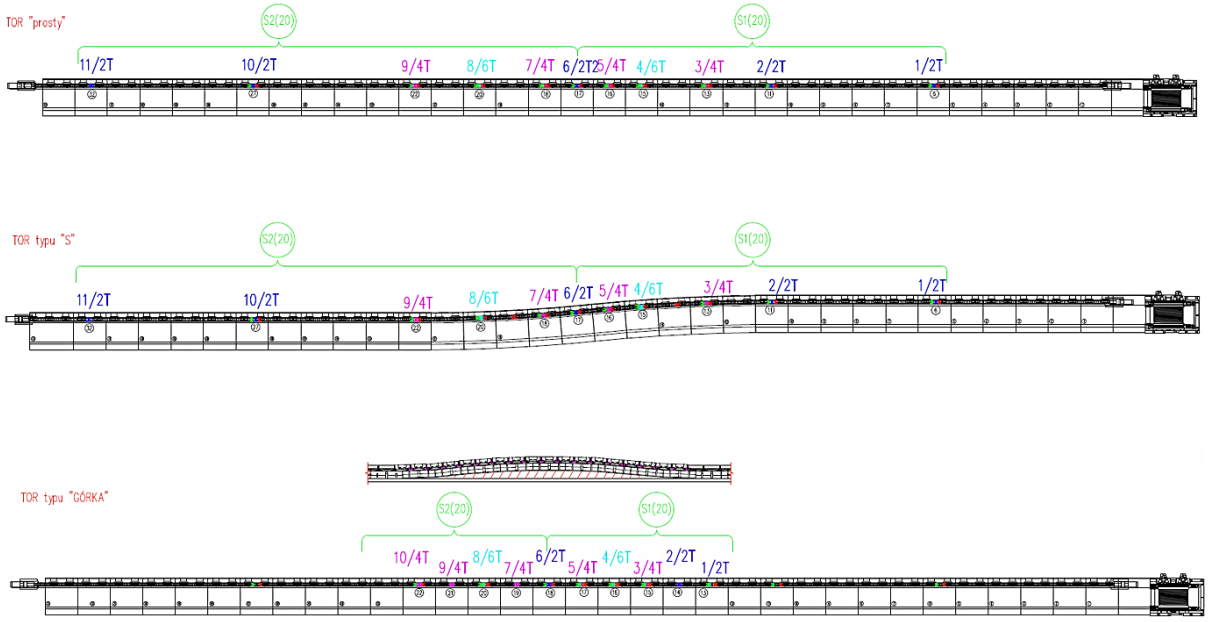

Fig. 13 Diagram of the arrangement of toothed segments on each type of track

For each type of track (P, S, and G), strain gauge tests were planned on two stands located approximately halfway along the track. To identify each type of toothed segment, markings were used, including the number of strain gauges attached to the segment and the sequential number of the measuring point (for example, 3/4T indicates the third measuring point with four strain gauges attached to the segment). During each test run, simultaneous recording (on a common timeline) of the signals from twenty-two strain gauges, along with the pressure signals in the tensioning system (at the beginning and end of the test track), the load force on the shearer, and the shearer's electrical parameters (current), were planned.

According to the art of strain gauge measurements, temperature compensation was also implemented. For this purpose, plates with compensation strain gauges were prepared (Fig. 14) (Roliński, 1981; Hoffman, 1989; Jung, 2022; Kitchin, 2004), the number of which corresponded to the number of strain gauges installed on the toothed segment. The prepared compensation plates, similarly to the toothed segments, were protected against moisture using an adhesive and silicone coating.

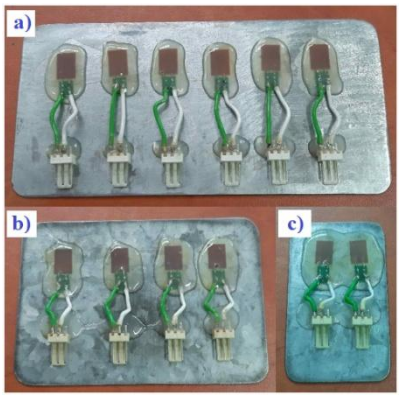

Rys. 14. Plates with compensation strain gauges corresponding to toothed segments covered with strain gauges in the following numbers: a) six, b) four, c) two

To verify the accuracy of the manufactured test pieces of toothed segments with attached strain gauges, the research team tested individual pieces on a testing machine (Fig. 15).

Fig. 15. Preliminary tests of toothed segments with attached strain gauges on a testing machine

Selected segments were subjected to compression tests to determine stress at the strain-gauge locations. These tests were intended to ultimately verify the segments' correct manufacture before submitting them for functional testing. Test loads on the toothed segments demonstrated the correct installation of the strain gauges and confirmed the ability to record strain values. As a result of applying a compressive force, strain values were recorded, and after removing the force, the strain gauges returned to their initial values. This confirmed the correct installation of the strain gauges and their operation within limits that did not cause permanent deformation.

Tests using the resistance strain gauges

Toothed segments, covered by strain gauges, were installed in the selected locations along the track, including straight sections P and areas of straightness distortion resulting from deflections in the horizontal plane S and vertical plane G. Figure 16 shows examples of the installation of all three types of toothed segments with two, four, and six attached strain gauges. All signal cables were led outside the track using the process holes in the guide base (Fig. 17).

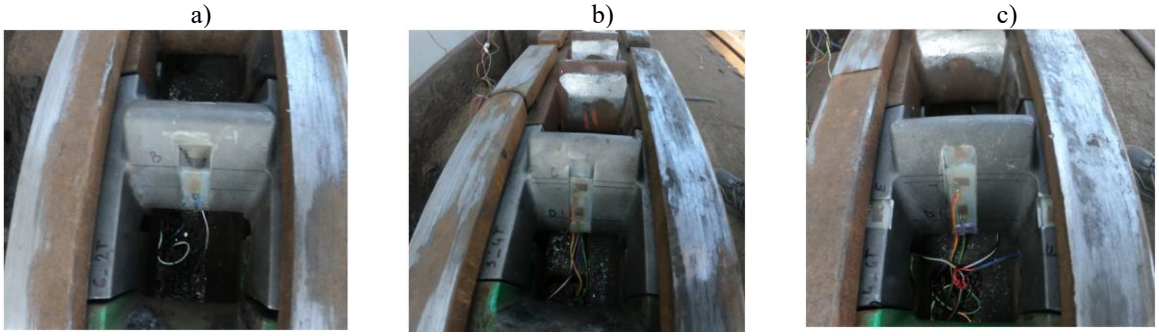

Fig. 16. Toothed segments installed on a test stand with the following number of strain gauges: a) two, b) four, c) six

Figure 17 also shows the location of the measuring toothed segment installed along the longwall complex, with the marking of the shearer's travel directions (with and without a load).

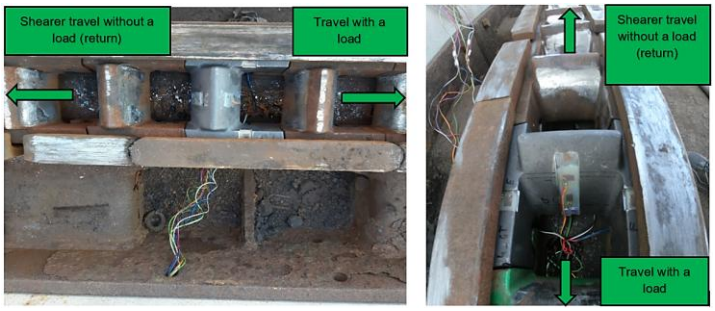

Fig. 17. Method of routing signal cables after installing the toothed segments with strain gauges glued in the guide

Each measuring line (active strain gauge on the toothed segment and compensating strain gauge) in the form of a half-bridge system (with one active strain gauge) was connected to a data acquisition and recording system consisting of a set of three SPIDER-8 amplifiers and a PC recording computer installed in a mobile measuring station. (Fig. 18).

Fig. 18. Mobile measuring station enabling recording and archiving of the data during strain gauge tests.

Toothed segments with attached strain gauges enabled the measurement and recording of the deformation of the material beneath the strain gauges and in their immediate vicinity as a result of the shearer's travel. Based on the identified material deformation state, it was possible to determine the stresses at the moment of contact between the gear wheel tooth and the flank of the toothed segment. Examples of the parameter curves recorded during the strain-gauge tests (stress, pressure, force, and electrical power) are shown in Fig. 19.

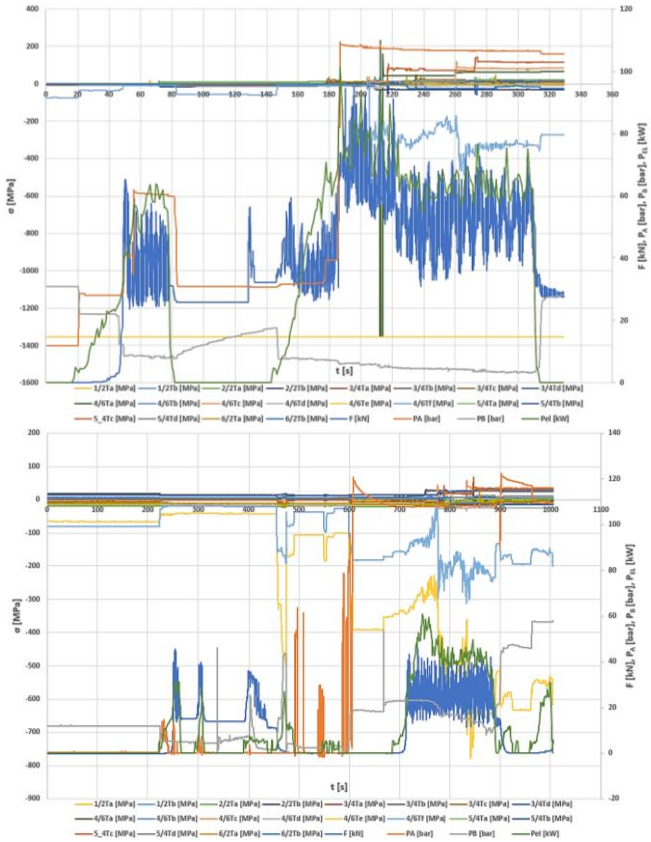

Fig. 19. Examples of parameters recorded during the strain gauge tests.

Test results analysis

As part of the KOMTRACK project, a series of tests and computer simulations were conducted, described in (Kotwica et al., 2019; Kalita, 2019; Kalita et al., 2020). Analyses of the test results and simulations of the longwall shearer advance system formed the basis for planning the tests using the resistance strain gauges described in this paper. During the tests, care was taken to ensure that the recorded current parameters, system loads, and strain gauge responses were aligned on a common time axis. This approach enabled analysis of the test results, assessment of the suitability of the applied method for determining the mating friction pair stresses, and determination of these stresses. As shown in Fig. 19, the amount of recorded measurement data on a common time axis appears chaotic. This is the response of each strain gauge to the load induced by the gang wheel's passage, as well as the current parameters and the force loading the shearer. A deeper analysis of the measurement data and the separation of each signal enabled the determination of stress values at the strain gauge locations. The presented curves show that each time the gang wheel contacts a toothed segment (a toothed segment with strain gauges attached), there is a momentary increase in compressive stresses on the side of contact between the two teeth and tensile stresses on the opposite, unloaded side of the tooth. Example stress curves, determined based on the strain gauge tests, are shown in Fig. 20 and Fig. 21.

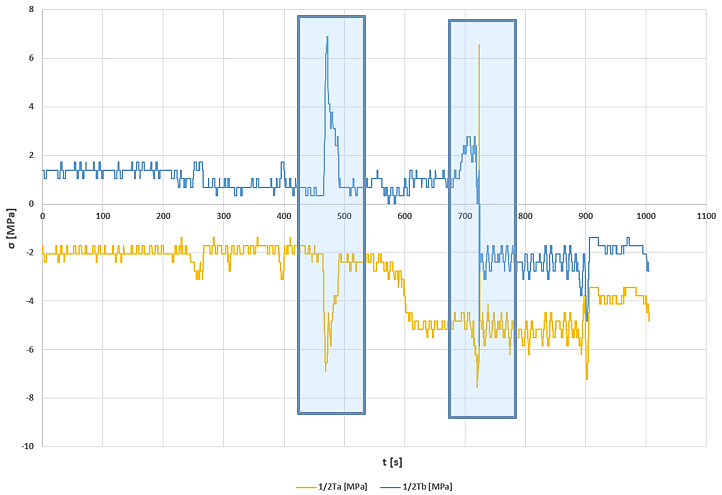

Fig. 20. Sample stress values determined for a toothed segment with two strain gauges attached.

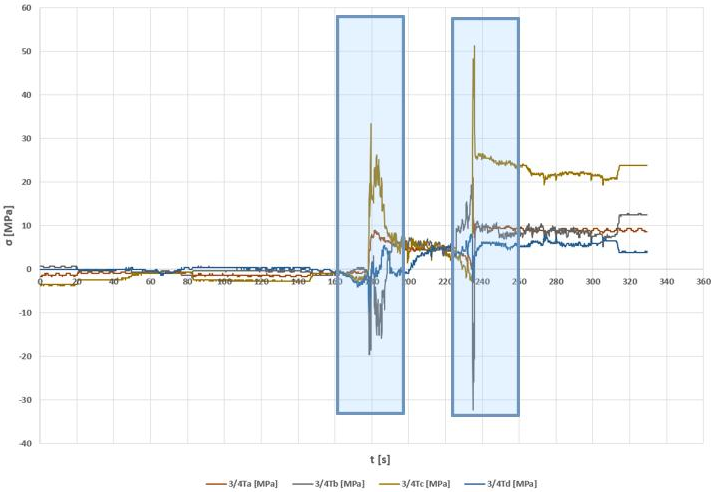

Fig. 21. Sample stress values determined for a toothed segment with four strain gauges attached

The frames indicate the portions of the graphs that correspond to the instant of contact between the gang wheel and the flank of the toothed segment. Positive stress represents the response of the strain gauge attached to the side, where the flank of the gang wheel tooth contacts the flank of the toothed segment. Negative values represent the response of the strain gauge installed on the other (unloaded) side of the toothed segment.

As mentioned earlier, during the tests, the shearer was loaded with a force generated by the winch braking system. Figure 22 shows an example graph of the force recorded during the shearer travel. The recorded load varied from 45 kN to 90 kN. The average load to the shearer was 63.5 kN.

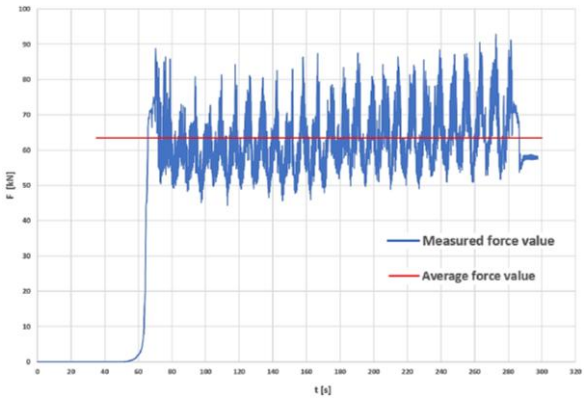

Fig. 22 Graph of the recorded load force on the shearer and its average value

During the tests, the shearer moved both loaded and unloaded, covering a route with strain gauges installed on toothed segments. Figure 23 shows sample stress graphs determined for toothed segments with two strain gauges attached.

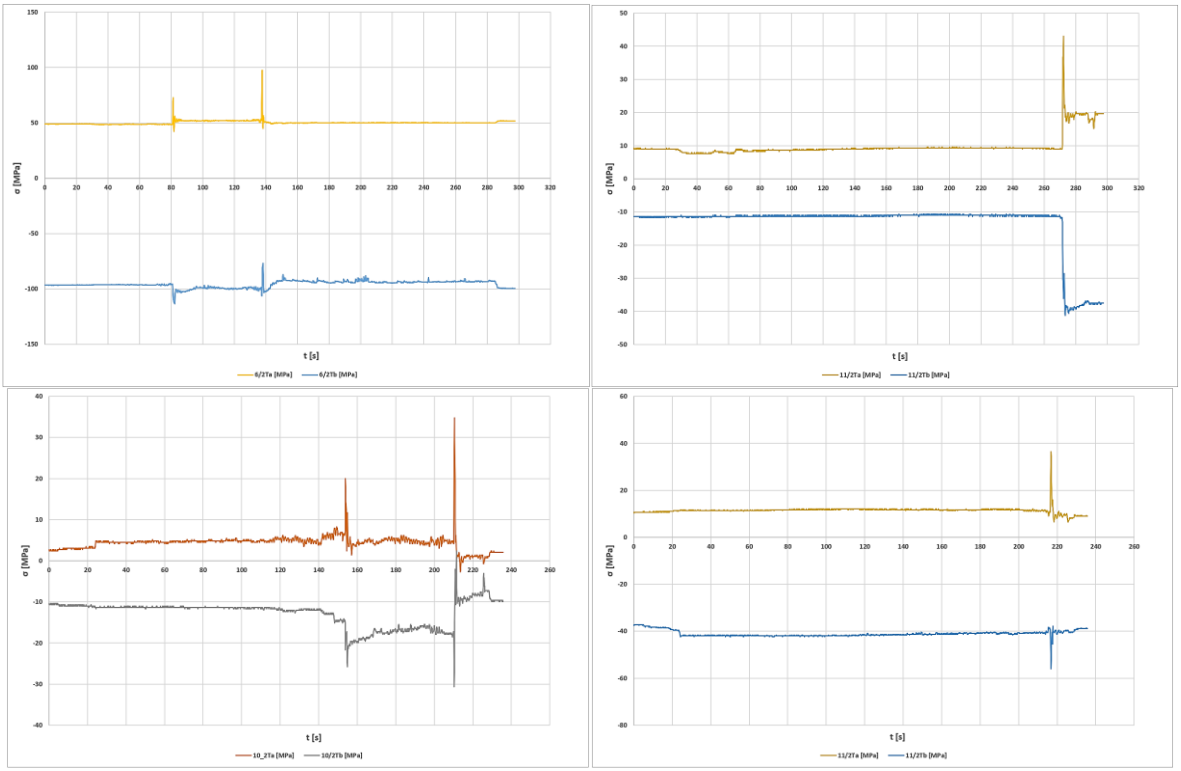

Fig. 23 Compressive and tensile stress diagrams determined for toothed segments with two strain gauges attached

Figures 24 and 25 show stress determined based on strain gauge tests for several selected toothed segments. As shown in the graph, the determined stress values due to shearer braking are approximately 20%-35% (27% on average) higher than the stresses generated on the toothed segment loaded by the shearer gang wheel while traveling unloaded.

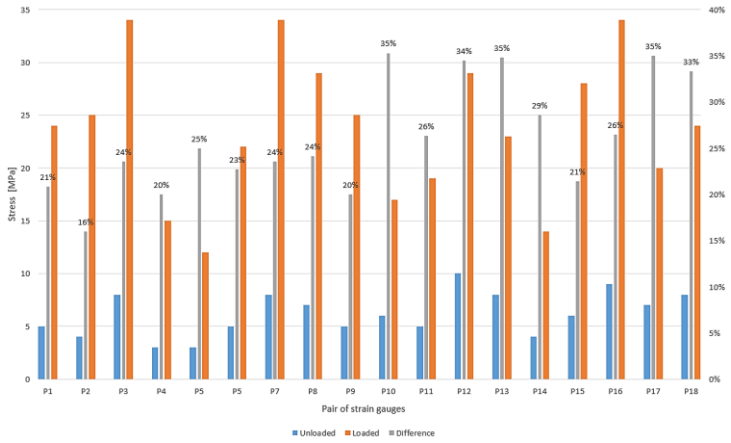

Fig. 24. Stresses resulting from the action of the first wheel on the toothed segment of the advance system – the case of the shearer traveling with and without a load

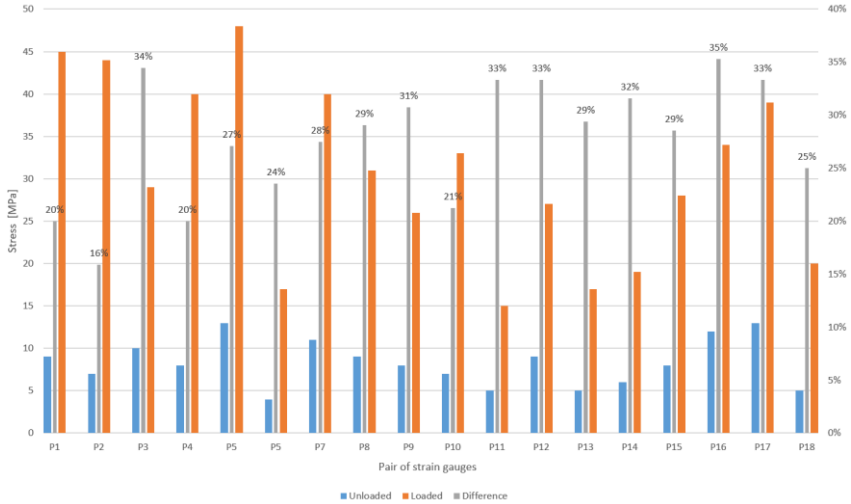

Fig. 25. Stress generated by the action of the second gear on the toothed segment of the advance system – the case of a loaded and unloaded shearer travel.

The test also included an analysis of stresses determined based on deformations recorded by strain gauges installed on the same toothed segment, on opposite sides of the tooth. Fig. 26 presents the stress for a loaded (braked) shearer run, while Fig. 27 presents the stress values for an unloaded shearer run.

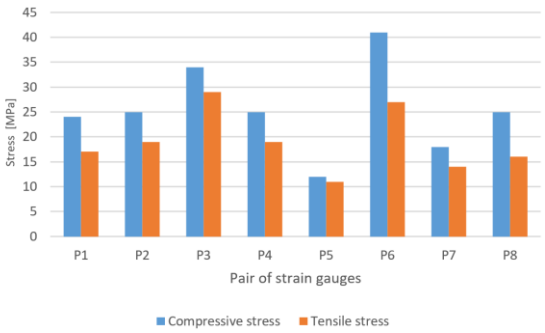

Fig. 26. Stresses in the shearer when travelling with a load

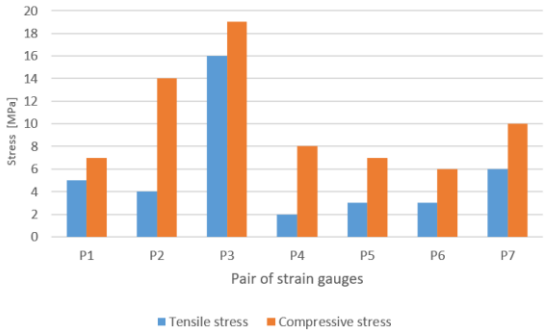

Fig. 27. Stresses in the shearer when travelling without a load

Based on the results, it was found that during the shearer run under load (Fig. 26), the compressive stresses generated by the gang wheel are higher than the tensile stresses on the opposite side of the tooth. A similar situation occurs when the shearer runs without a load. In this case, the change in travel direction causes compressive and tensile stresses on the opposite sides of the toothed segment than during the run with a load, while the determined values are lower. Compressive and tensile stresses, determined based on the deformations recorded by pairs of strain gauges installed on the same tooth, are illustrated in Fig. 23. This stress state is indicated by negative values (in the direction of action) of compressive stresses and positive values of tensile stresses. The identified relationships confirm that the applied testing method and the adopted simplifications in tooth geometry, which

enabled the attachment of strain gauges, enable the determination of stress in the tooth of a toothed segment of a longwall shearer advance system subjected to bending. Stress values were determined similarly for toothed segments with four strain gauges attached. Example graphs of the determined compressive stresses and the corresponding tensile stresses are shown in Fig. 28.

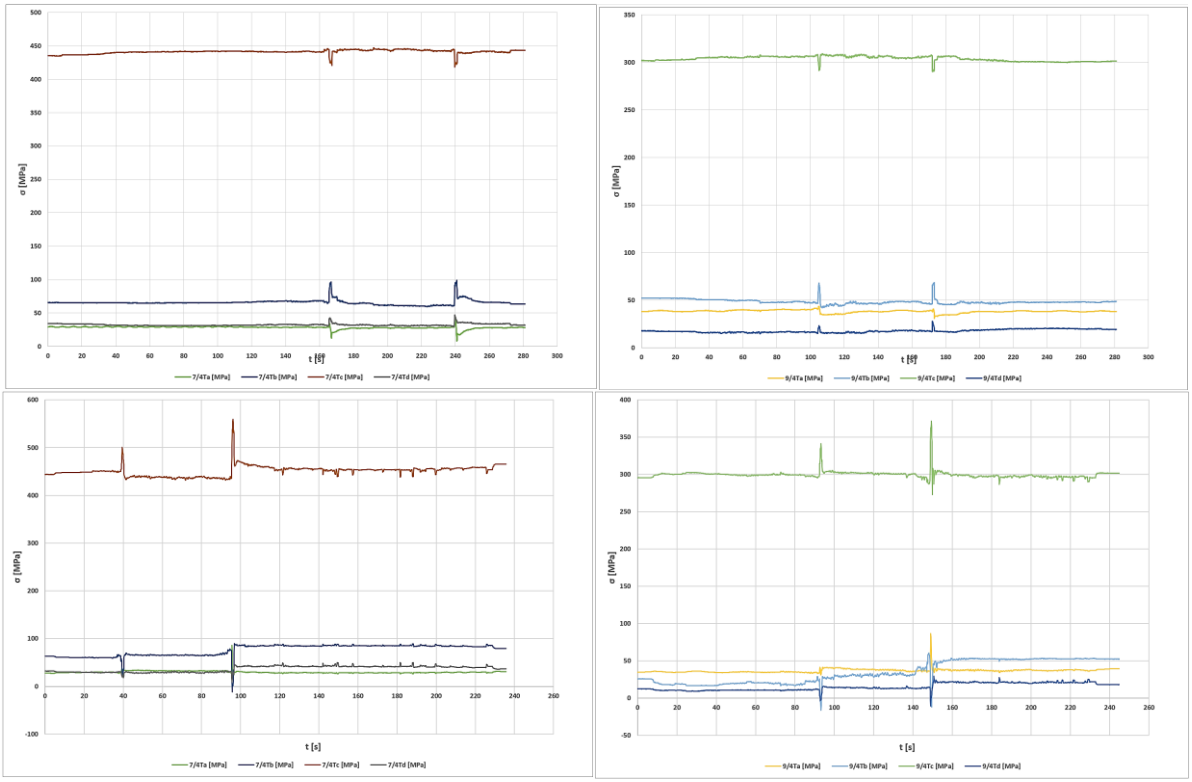

Fig. 28. Compressive and tensile stress graphs determined for toothed segments with four strain gauges attached.

The stress values for each strain gauge are given in Fig. 29-32. In this case, the determined stresses generated at the locations of strain gauges "a," "b," "c," and "d" as a result of the shearer-loaded run are higher than the stresses determined for the unloaded run. As with the toothed segments with two strain gauges attached, the difference between the stress values is similar, ranging from 28% to 30% (average 29%).

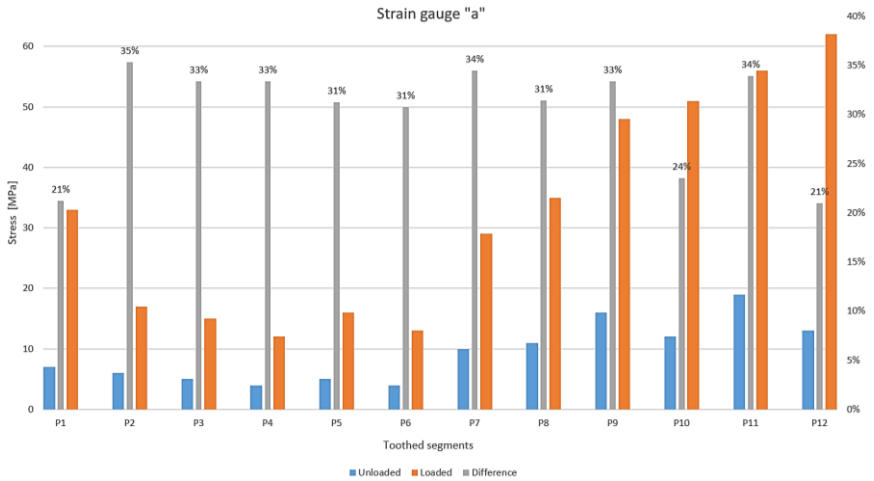

Fig. 29. Stresses generated at the place of attachment of the strain gauge "a" as a result of driving the shearer under a load and without load

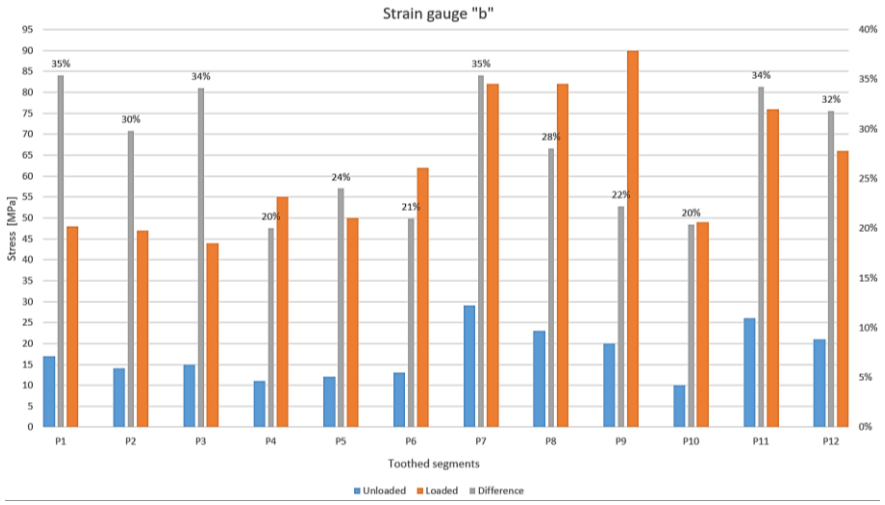

Fig. 30. Stresses generated at the place of attachment of the strain gauge "b" as a result of driving the shearer under a load and without a load

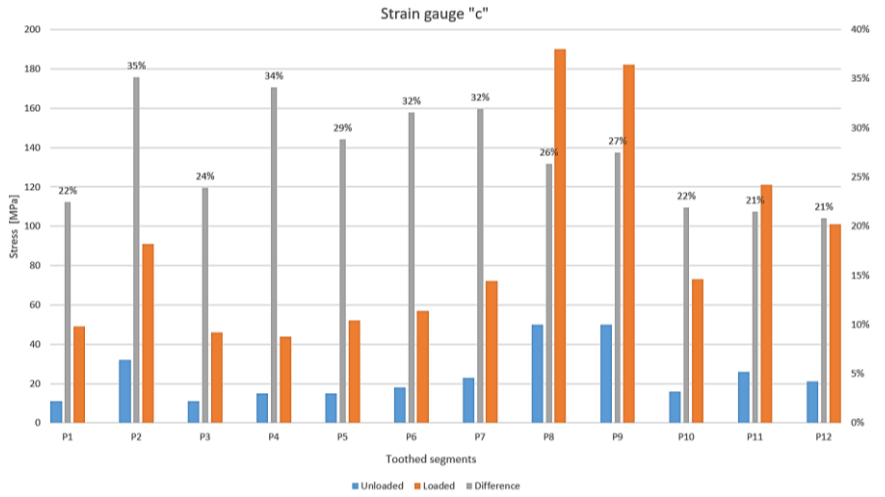

Fig. 31. Stresses generated at the place of attachment of the strain gauge "c" as a result of driving the shearer under a load and without a load

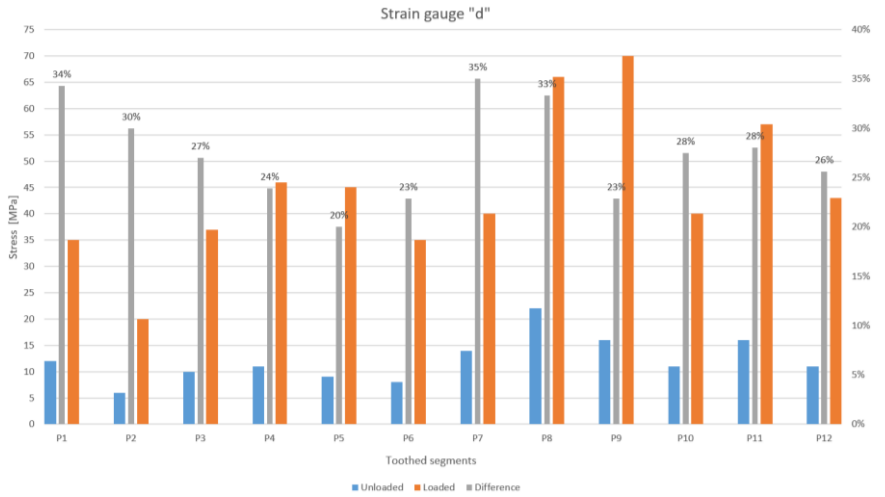

Fig. 32. Stresses generated at the place of attachment of the strain gauge "d" as a result of driving the shearer under a load and without a load

Based on the results, it was also possible to analyze the stress for strain gauge pairs "a"–"c" and "b"–"d" installed at different heights on the tooth flank of the toothed segment, on opposite sides. The results are illustrated in Fig. 33 and Fig. 34.

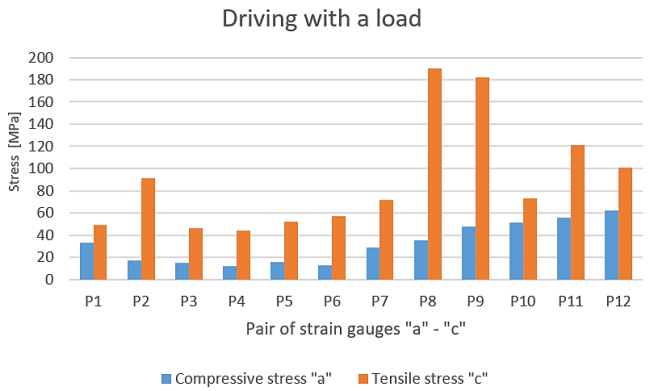

Fig. 33. Comparison of stress values determined for the places of the strain gauges "a" and "c" - upper part of the toothed segment flank

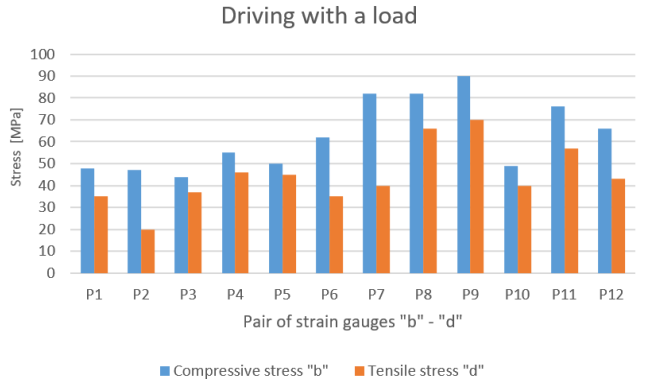

Fig. 34. Comparison of stress values determined for the places of gluing the strain gauges "b" and "d" - lower part of the toothed segment flank

Pair of strain gauges "a"–"c" measured strains in the upper part of the toothed segment flank, while pair "b"–"d" was placed in the lower part, at the base (Fig. 11). Depending on the strain gauge location, the results differ in magnitude and direction of action. The stresses determined based on measurements for strain gauge "a" are of tensile nature, and their values are lower than those determined for the counterpart "c," for which the stresses are of compressive nature. The stresses determined based on data recorded by strain gauges "b"–"d" are identical in nature, although their values differ. As the tooth in the toothed segment is thicker at the bottom (at the base), compressive stresses are higher than the tensile stresses determined on the opposite side of the toothed segment. The identified stress state confirms that less deformation occurs in the lower part of the tooth than in its upper part.

As mentioned in the introduction, the developed test stand and testing methodology allowed for carrying out the tests on the straight track P (Fig. 6), S (Fig. 7), and G (Fig. 8). Based on the collected data, the stress values generated at the locations where strain gauges "a," "b," "c," and "d" were attached for loaded shearer travel on track P and G (Fig. 35-38) were compared.

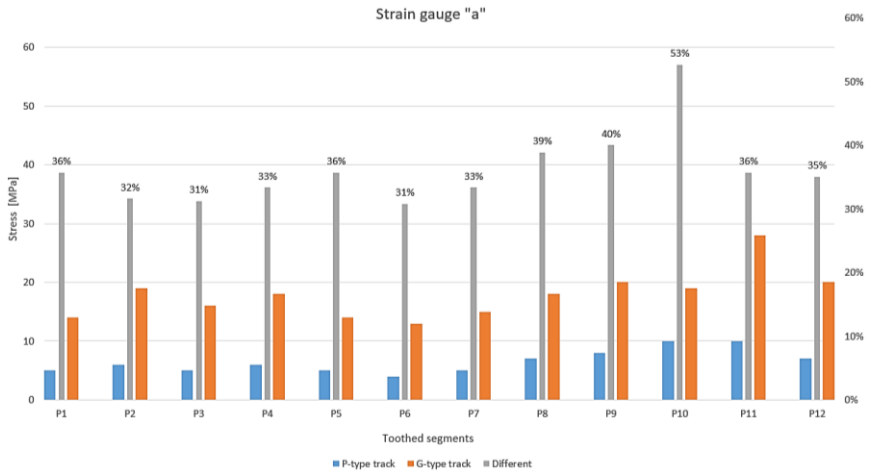

Fig. 35. Comparison of stress at the place of the strain gauge "a" when the shearer is driven on the P and G type track.

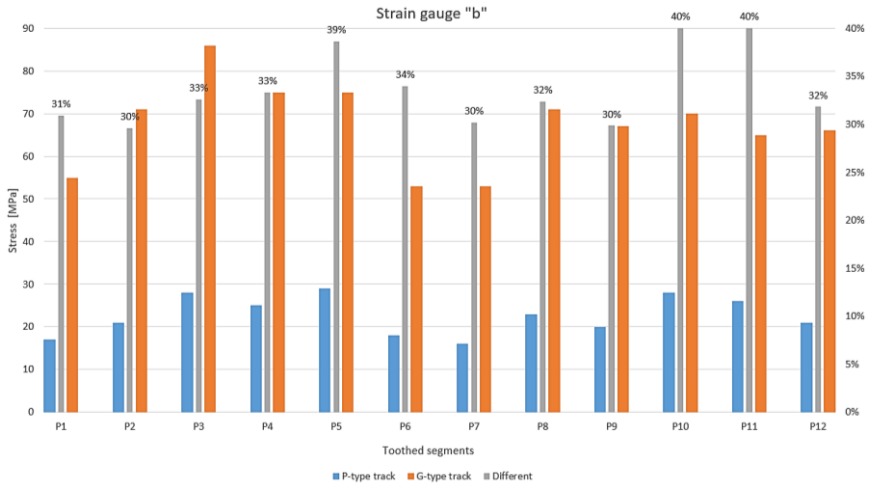

Fig. 36. Comparison of stress at the place of the strain gauge "a" when the shearer is driven on the P and G type track.

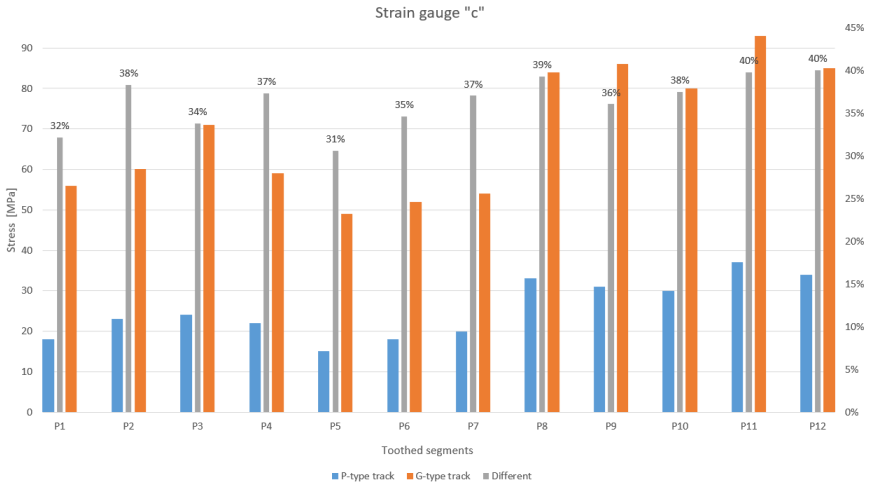

Fig. 37. Comparison of stress at the place of the strain gauge "c" when the shearer is driven on the P and G type track

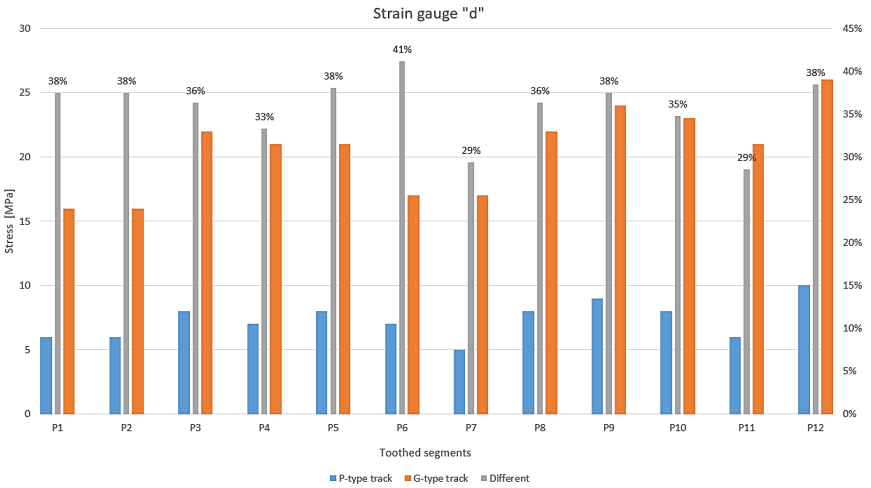

Fig. 38. Comparison of stress at the place of the strain gauge "d" when the shearer is driven on the P and G type track

This article does not consider the test results for track S. As expected, the determined stress at each analyzed location is higher for travel on track G than for track P. Repeatability of the results was observed for both loaded and unloaded travels. Furthermore, there was a high degree of compliance in the difference between the determined stress values, which averaged 35% across each strain gauge.

Conclusions

The innovative shearer advance system, developed as part of the KOMTRACK project (contract no. POIR.04.01.04-00-0068/17), is characterized by the flexibility and the ability of the toothed segments to continuously adjust (keeping pace with load and the changing geometry of the face conveyor route) to the shearer gang wheel. This functionality, a distinctive feature compared to other shearer advance systems, was achieved through the special design of the guides and toothed segments. The project, co-financed by the European Regional Development Fund, provided an excellent opportunity for a series of functional, engineering, and material tests using various testing technologies. Resistance strain gaging is one of the testing technologies. With regard to the testing facility, which is designed for operation in harsh mining conditions in areas at risk of methane and/or coal dust explosions, the only possible location for this type of test was a test (laboratory) stand constructed on the surface storage yard of the Piast-Ziemowit Coal Mine (Ruch Piast).

Within the framework of the research work opportunities, the KOMAG Institute attempted to use resistance strain gauges to determine approximate values of the stresses generated at the contact surface between a toothed segment and the flank of a gear wheel tooth, and to verify the strength of the mating friction pair. For this purpose, special toothed segments were developed and manufactured, allowing for the attachment of strain gauges to their surfaces.

During the tests, successive travels of the longwall shearer along the P, S, and G tracks were made. The results of tests using resistance strain gauges to measure shearer travel along the P and G tracks with toothed segments, with two and four strain gauges, were presented. During outward travel, braking force was simulated, and during return travel, the shearer operated without a load. As a result of the tests, a large amount of measurement data was collected, including strain-gauge responses, braking force, pressure in the track-tensioning system, and shearer electrical parameters.

The tests allowed us to determine the stresses generated near the friction pair contact surface as a function of the constant load applied to the shearer, and then compare the results with those for travel without a load. For obvious reasons, the determined stresses cannot be considered surface pressure values at the tooth flank, but they nevertheless provide an insight into the stress state resulting from the friction pair interaction. Furthermore, the tests confirmed the basic relationships between compressive stresses on the side of the applied load and tensile stresses on the opposite side of the tooth (tooth bending). High consistency and repeatability of the results were also observed, with values varying within a range of 20-30%. The tests indicate that the applied resistance strain gauge method is effective and can be used to identify stresses near the contact surface of the friction pair formed by the tooth of the gang wheel and the tooth of the toothed segment in the longwall shearer advance system. Stress determined from measured deformations of a single toothed segment yields repeatable results after more than 20 contacts between the gang wheel and the toothed segment. In some cases, a greater number of load cycles can cause decalibration of the strain gauge system, leading to increasing discrepancies in the results or a complete loss of measurement capabilities. During the tests, it was found that in several strain gauges, despite the required care and appropriate safeguards, the adhesive bond was damaged, and the strain gauge lost its measuring properties.

The tests with resistance strain gauges also allowed comparison of the measured stress results with those from numerical analyses using the finite element method. In the FEM calculations, when defining the boundary conditions, the values of the compressive forces on the toothed segments generated by the tensioning systems (determined on the basis of recording the pressure in the hydraulic cylinders) and the values of the shearer braking force applied by the hydraulic winch brake were used during the functional tests. Preliminary results of these analyses are presented in (Kotwica et al., 2023). FEM analyses of the toothed segments, taking into account the operating parameters of the advanced system recorded during the strain gauge tests, and their comparison, due to the complexity of the issues, will be the subject of a subsequent scientific article.

References

Braun, G. (1983). Chain Having Longitudal Stiffness Used with Hauling and Cutting Equipment. U.S. Patent 4,372,619.

Fennelly, S.D. (1978). Chainless Haulage Systems for Power Loaders: Information Circular as of April 1978; United States Department of Energy: Washington, DC, USA.

Fries, J. (2003). Rozwój bezcięgnowych systemów posuwu kombajnów ścianowych. *Uhli Rudy Geol. Pruzk,* 10, 22–24.

Giza, T. and Mann, R. (2005). Wpływ zużycia zębów koła napędowego i zmiany podziałki zębatki na charakter zazębienia i prędkość posuwu kombajnu. *Zeszyty Naukowe. Górnictwo / Politechnika Śląska*, 269, 407–416. (In Polish)

Giza, T., Sobota, P. and Mann, R. (2003). Wpływ zazębienia koła napędowego z zębatką sworzniową mechanizmu posuwu BP na parametry posuwu kombajnu ścianowego. In Proceedings of the Konferencja KOMTECH

Nowoczesne, Niezawodne i Bezpieczne Systemy Mechaniczne w Świetle Wymagań Unii Europejskiej, Szczyrk, Poland, 17–19 November, 189–197. (In Polish)

Gondek, H., Marasova, D. and Fries, J. (2000). Możliwości zwiększenia trwałości zazębienia koła napędowego z zębatką mechanizmu bezcięgnowego posuwu kombajnu ścianowego. In Proceedings of the TEMAG 2000, *Trwałość elementów i węzłów konstrukcyjnych maszyn górniczych*, VIII Konferencja Naukowo-Techniczna, Gliwice - Ustroń, 25-27 October, 73-80. (in Polish)

Hoffman, K. (1989). An Introduction to Measurement using Strain Gauges, Hottinger Baldwin Messtechnik GmbH, Darmstadt.

Huang, K. J. and Su, C. Y. (2013). An investigation on helical gear pair stresses incorporating misalignment and detail modification. *Journal of Vibroengineering*, vol. 15, No. 1, 90–99.

Iriarte, X., Aginaga, J., Gainza, G., Ros, J., and Bacaicoa J. (2021). Optimal strain-gauge placement for mechanical load estimation in circular cross-section shafts. *Measurement*, vol. 174, April, https://doi.org/10.1016/j.measurement.2020.108938

Jung, W. G. (2005). Op Amp Applications Handbook, Analog Devices USA.

Kalita, M. (2019). Designing process of a toothed segment of the KOMTRACK haulage system. *New trends in production engineering,* vol. 2, Issue 1, 121-129. DOI 10.2478/ntpe-2019-0013

Kalita, M., Mazurkiewicz, A., Pieczora, E. and Tarkowski, A. (2020). KOMTRACK – nowej generacji system posuwu wysokowydajnych kompleksów ścianowych – wstępne prace projektowe. *Mechanizacja, Automatyzacja i Robotyzacja w Górnictwie.* Monografia, Wydawnictwa AGH, Kraków, 23-31. ISBN 978-83-66364-62-2

Kitchin, Ch. and Counts, L. (2004). A Designer's Guide to Instrumentation Amplifiers, Analog Devices USA.

Korski J. (2021). Longwall shearer's haulage systems - a historical review. Part 1 – cable haulage systems. *Mining Machines*, vol. 39, Issue 1, 17-27. DOI: 10.32056/KOMAG2021.1.2

Korski, J. (2021). Longwall shearer haulage systems - a historical review. Part 2 - First cordless haulage systems solutions. *Mining Machines*, vol. 39, Issue 2, 39, 24–33. https://doi.org/10.32056/KOMAG2021.2.3

Korski, J. (2020). Capacity Losses Factors of Fully Mechanized Longwall Complexes. *Mining Machines*, No. 3, 12-21. DOI: 10.32056/KOMAG2020.3.2

Kotwica, K., Stopka, G., Wieczorek, A.N., Kalita, M., Bałaga, D. and Siegmund, M. (2023). Development of Longwall Shearers' Haulage Systems as an Alternative to the Eicotrack System Used Nowadays. *Energies*, No. 16(3), 1402, 1-19, DOI:10.3390/en16031402

Kotwica, K., Stopka, G., Kalita, M., Bałaga, D. and Siegmund, M. (2021). Impact of Geometry of Toothed Segments of the Innovative KOMTRACK Longwall Shearer Haulage System on Load and Slip during the Travel of a Track Wheel. *Energies*, vol. 14(9), 2720. https://doi.org/10.3390/en14092720

Kotwica, K., Stopka, G. and Gospodarczyk, P. (2019). Simulation tests of new solution of the longwall shearer haulage system, Scientific and Technical Conference on Innovative Mining Technologies (IMTech), Innovative Mining Technologies (Imtech), Pt 2.

Kovanic, L., Ambrisko, L., Marasova, D., Blistan, P., Kasanicky, T., Cehlar, M. (2021). Long-Exposure RGB Photography with a Fixed Stand for the Measurement of a Trajectory of a Dynamic Impact Device in Real Scale*. Sensors, 21(20).* DOI 10.3390/s21206818

Kovanič, Ľ., Štroner, M., Blistan, P., Urban, R., & Boczek, R. (2023). Combined ground-based and UAS SfM-MVS approach for determination of geometric parameters of the large-scale industrial facility – Case study. *Measurement*, *216*, 112994. https://doi.org/10.1016/j.measurement.2023.112994.

Langefeld, O. and Paschedag, U. (2019). Longwall Mining—Development and Transfer. *Mining Report—Glückauf*, 1, vol. 155.

Lingaiah, K. and Ramachandra, K. (1977). Three-dimensional photoelastic study of the load-carrying capacity/face width ratio of Wildhaber-Novikov gears for automotive applications. *Experimental Mechanics,* 17, 392–397.

Link, H., Keller, J. and Guo, Y. (2013). Gearbox Reliability Collaborative Phase 3 Gearbox 2 Test Plan Technical Report NREL/TP-5000-58190.

Lisle, T.J., Shaw, B.A. and Frazer, R.C. (2017). External Spur Gear Root Bending Stress: A Comparison of ISO 6336:2006, AGMA 2101-D04, ANSYS Finite Element Analysis and Strain Gauge Techniques. *Mechanism and Machine Theory*, 111(11), 1–9. DOI:10.1016/j.mechmachtheory.2017.01.006

Lisle, T.J., Shaw, B.A. and Frazer, R.C. (2018). Internal Spur Gear Root Bending Stress: A Comparison of ISO 6336:1996, ISO 6336:2006, VDI 2737:2005, AGMA, ANSYS finite element analysis and strain gauge techniques. *Proc. Inst. Mech. Eng. Part C J. Mech. Eng. Sci.,* 233(5), 1713–1720. DOI:10.1177/0954406218774364

Li, S., Zuo, S., Luo, Y. and Huang, Z. (2023). An improved load distribution model for involute helical gear pairs considering an actual contact ratio. *Proceedings of the Institution of Mechanical Engineers, Part C: Journal of Mechanical Engineering Science*, vol. 237, Issue 21, 5174 – 5186. DOI:10.1177/09544062231157230

Mackie K. and Fimemme, T.E. (1987). Design & Development of Longwall Shearers for Overseas Application. *Advances in Mining Science and Technology*m, 1, 169–188.

Matsui, K. and Shimada, H. (1996). Control of stability of retreat longwall gate road. *Mining Science and Technology,* vol. 7, 709-713.

Park, J. H., Chung, W. J, Park, Y. J., Kim, H. S., Seo, J. N. and Park, J. S. (2024). Effect of Rim and Web Thickness on Tooth Root Stress of Spur Gear. *Int.J Automot. Technol.*, 25, 279–293.

Paucker, T., Otto, M. and Stahl, K. (2019). Determining the load distribution by measuring the tooth root stresses. *Forsch Ingenieurwes,* vol. 83, 621–626. https://doi.org/10.1007/s10010-019-00349-2

Piekło, J., Maj, M., Żuczek, R. and Pysz, S. (2016). Assessment of Durability of the Toothed Segment Based on FEM Analysis and Low Fatigue Cycle Test. *Arch. Foundry Eng.,* 16, 113–118.

Raghuwanshi, N. K. and Parey, A. (2016). Experimental measurement of gear mesh stiffness of cracked spur gear by strain gauge technique. *Measurement*, vol. 86, 266-275, https://doi.org/10.1016/j.measurement.2016.03.001

Roliński, Z. (1981). *Tensometria oporowa. Podstawy teoretyczne i przykłady zastosowań*. WNT, Warszawa.

Sikora, W., Giza, T. and Mann, R. (2023). Wpływ przegięcia trasy przenośnika zgrzebłowego na współpracę koła napedowego z zębatką bezciegnowego systemu posuwu typu BP. In Proceedings of the TUR 2003*, III Międzynarodowa Konferencja Techniki Urabiania 2003*, Kraków-Krynica, Poland, 23–26 September, 151–159. (In Polish)

Sikora, W., Dolipski, M., Osadnik, J. and Remiorz, E. (2005). Analiza geometryczna wybranych elementów układu ciągnienia 2BP. *Zeszyty Naukowe. Górnictwo / Politechnika Śląska*, 269, 543–551. (In Polish)

Syzrantsev, V. and Syzrantsev, K. (2017). Determination of stresses in tooth roots of gears by Integral Strain Gauges. *Advances in Engineering Research*, vol. 133, *Actual Issues of Mechanical Engineering*.

Twardoch, K., Grzesica, P. and Nawrat, A. (2016). Analiza współpracy koła napędowego z zębatką¸ o owalnym przekroju sworzni w mechanizmie posuwu EICOTRACK (2BP). In Proceedings of the TEMAG 2016, XXIV Międzynarodowa Konferencja Naukowo-Techniczna, *Trwałość Elementów i Węzłów Konstrukcyjnych Maszyn Górniczych*, Ustroń, Poland, 3–5 November, 291–304. (In Polish)

Zachura, A. and Żuczek, R. (2014). System Posuwu Flextrack Zwiększający Trwałość i Niezawodność Napędu Kombajnu Ścianowego. *Innowacyjne Techniki i Technologie dla Górnictwa. Bezpieczeństwo-Efektywność-Niezawodność*, KOMTECH, ITG KOMAG, Gliwice, Poland, 151–161. (In Polish)

Zuo, S., Sun, Y., Chen, L., Li, S., and Wang, M. (2025). Calculation Method and Experimental Investigation of Root Bending Stress in Line Contact Spiral Bevel Gear Pairs. *Machines*, 13(8), 632. https://doi.org/10.3390/machines13080632